Electronic Supplementary Material: Supplemental Methods and Results

“Rapid evolution rescues hosts from competition and disease but—despite a dilution effect—increases the density of infected hosts”

Alexander T. Strauss[1,2] (straussa@umn.edu), Jessica L. Hite[1,3] (jhite2@unl.edu), Marta S. Shocket[1,4] (mshocket@standford.edu), Carla E. Cáceres[5] (cecacere@illinois.edu), Meghan A. Duffy[6] (duffymeg@umich.edu), and Spencer R. Hall[1] (sprhall@indiana.edu)

[1]Department of Biology, Indiana University, Bloomington, IN 47401, USA

[2]Present address: Department of Ecology, Evolution, and Behavior, University of Minnesota, St. Paul, MN 55108, USA

[3]Present address: Department of Biological Sciences, University of Nebraska at Lincoln, Lincoln, NE 68588, USA

[4]Present address: Department of Biology, Stanford University, Stanford, CA 94305

[5]School of Integrative Biology, University of Illinois at Urbana-Champaign, Urbana, IL 61801, USA

[6]Ecology and Evolutionary Biology, University of Michigan, Ann Arbor, MI 48109, USA

SUPPLEMENTAL METHODS

We begin by describing details of the assays for trait measurements, setup logistics for the mesocosm experiment, and genotyping protocols. Then we describe our model selection criteria for repeated measures mixed models (predicting changes in genotype frequencies and mean focal host traits).

Trait Measurements

Methods for trait measurements are identical to Strauss *et al.* (in revision). Prior to trait measurement assays, all isoclonal lines were fed high densities of high quality laboratory-cultured algae (2.0 mg mass/L *Ankistrodesmus falcatus*). Cultures were maintained in high hardness COMBO (artificial lake water media) under ideal conditions for three generations, in order to standardize any maternal affects.

Susceptibility: We calculated an index of susceptibility (the transmission coefficient, β) for each isolonal line using infection assays. Susceptibility represents the probability of a focal host becoming infected, given density of infectious spores (Z), the duration of spore exposure (t), and body length of the focal host (L). Transmission depends on body length, because larger hosts encounter parasites at a higher foraging (i.e., exposure) rate (Hall *et al.* 2007). For the assay, we first reared cohorts of neonates of each isoclonal line (fed 1.0 mg mass/L/day of highly edible algal food, *Ankistrodesmus*). After 5 days, individuals were isolated in 15 mL of media. Fifteen of these individuals were exposed to each of three densities of fungal spores (Z): 75, 200, or 393 spores/mL. Spores (< 6 weeks old) were all reared in a standard focal host genotype. After ~8 hours of exposure time (t), we measured body length of all individuals (L) with a dissecting microscope and micrometer. Thereafter, we transferred each individual to a fresh 50 mL tube of media daily, until death. Dead individuals were visually inspected with a

dissecting microscope to diagnose infection. Individuals that died too early to determine infection were omitted from the analysis. This assay was conducted in three different experimental blocks, with 2 isoclonal lines repeated among blocks, in order to control for any block effects (due to potential variation in spore infectivity).

To estimate the transmission coefficient (β) from this transmission assay, we simplified a previously used mathematical model (e.g., Hall *et al.* 2007; Hall *et al.* 2012). This model assumes that the initial density of susceptible hosts in the assay (S_i; one per tube) decreases as susceptible hosts (S) contact spores (Z) at rate βL^2, where β is a transmission coefficient after controlling for size L^2 (proportional to surface area of the host). Specifically, $dS/dt = -\beta L^2 SZ$. Solving this equation for the final density of susceptible hosts (S_f), after exposure time (t), yields: $S_f = S_i \exp(-\beta L^2 Z t)$. We estimated the transmission coefficient (β) for each isoclonal line, using maximum likelihood and the BBLME package in R (Bolker 2008; R Core Team 2017). The binomial distribution (infected or not) served as the likelihood function. After controlling for block effects, we bootstrapped standard errors around each isoclonal line.

Competitive Ability: We calculated an index of competitive ability with juvenile growth rate assays on low resources (e.g., Hall *et al.* 2012). Mass accrual of neonates during a 5-6 day juvenile period becomes directly proportional to fitness once adults begin investing energy in reproduction (Lampert & Trubetskova 1996). In turn, competitive ability depends on fitness when resources are limiting (reviewed: Grover 1997). Thus, focal hosts with high juvenile growth rates on low food resources become strong competitors (Strauss *et al.* in revision).

To calculate juvenile growth rate, we first isolated cohorts of neonates (< 24 hours old) for each isoclonal line. We obtained initial day 0 mass measurements (m_i) by drying and weighing 6-13 neonates (mean N = 9.3 per isoclonal line) with a Mettler microbalance (Mettler-Toledo, Columbus, Ohio, USA). We also placed live neonates (mean N = 16.6) in separate 50 mL tubes of media. Each day, we transferred these individuals into fresh media (fed 0.15 mg

mass/L *Ankistrodesmus* daily). Then, after 5-6 days (*d*), we dried and weighed them, yielding final mass estimates (m_f). With these data, we calculated juvenile growth rate on low resources (*GR*) as the mean for each combination of initial and final mass estimates: $GR = [\ln(m_f) - \ln(m_i)] / d$. Finally, we bootstrapped standard errors around means for each genotype in R.

Mesocosm Experiment

Our mesocosm experimental design crossed standing focal host trait variation (constrained [-V] or variable [+V]) with presence/absence of parasites (+/- P) and competitor/diluters (+/- C). Each replicate was housed in a 75-liter acid-washed polyethylene tanks in a climate-controlled room and grown under a 16 L: 8 D light cycle. We began preparing tanks by filling them to 60 liters with high-hardness COMBO (artificial lake water). Then, we added initial doses of nitrogen and phosphorus in the form of sodium nitrate and potassium phosphate (300 ug L^{-1} N as $NaNO_3$ and 20 ug L^{-1} P as K_2HPO_4). We replaced evaporated COMBO and replenished 5% of the initial nutrient dose per day (assuming exponential loss), throughout the experiment. Finally, we inoculated the tanks with 50 mg dry weight of *Ankistrodesmus falcatus*, and let this algae grow for two days prior to adding any focal hosts.

Next, we added focal hosts to the experiment. Each clonal line of focal hosts was reared in monoculture tanks, where they reached different densities. We estimated their final densities by sampling in triplicate. We added a fixed volume from each monoculture tank to the appropriate experimental tanks. Genotypic identities of the eight genotypes featured in (Strauss *et al.* in revision) are included here in brackets. Constrained populations received four isoclonal lines (mean density 2.1 hosts L^{-1}; total density 8.3 hosts L^{-1}), including “Dogwood 4” [G7] (2.5 L^{-1}), “Warner 5” [G4] (1.8 L^{-1}), “Bristol 112” [G5] (2.7 L^{-1}), and “A4-5” (1.2 L^{-1}). Variable populations received all ten isoclonal lines (mean density also 2.1 hosts L^{-1}; total density 21 hosts L^{-1}), including “Downing 282” [G1] (1.9 L^{-1}), “Midland 273” [G8] (1.3 L^{-1}), “Midland 263” [G6] (2.3 L^{-1}),

“Bristol 10” [G3] (2.2 L^{-1}), “Bristol 6” (0.9 L^{-1}), “Standard” (2.8 L^{-1}), “Dogwood 4” [G7] (2.5 L^{-1}), “Warner 5” [G4] (1.8 L^{-1}), “Bristol 111” [G2] + “Bristol 112” [G5] (4.1 L^{-1}), and “A4-5” (1.2 L^{-1}). “Bristol 111” and “Bristol 112” proved indistinguishable with our microsatellite markers and were treated as a single genotype. Finally, we did not have measurements of competitive ability for “A45,” “Bristol 6,” or “Standard” (not pictured in Fig. 1). We also did not have a measurement of susceptibility for “Standard.” However, these genotypes remained extremely rare in both monoculture (Strauss *et al.* in revision) and evolving populations. Hence their traits would have inconsequentially impacted our calculation for mean traits of the evolved focal host populations.

Finally, we added competitor/diluters (single genotype; 2.1 L^{-1}) on day 0 and parasites (5,000 L^{-1}) on day 21 to appropriate experiment tanks. In one tank, we detected a large spillover of disease into the competitor/diluter population. Since these infections fundamentally changed the ecological infection dynamics of this replicate, we omitted this tank from all analyses.

Genotyping

DNA Extraction: Individuals for genotyping were selected from preserved samples. If fewer than 10 individuals were available on days 25 and 70, we genotyped all of them (mean N = 8.2 per tank, per time). Overall, we genotyped 718 individuals. None were visibly infected, and adults were selected over juveniles when possible, since they yielded more DNA. First, we rinsed each individual in deionized water to remove ethanol. Then we digested tissue and extracted DNA by grinding (automatic pestle, 10 seconds) and incubating each individual in 60 µL proteinase-K extraction buffer (protocol modified from Schwenk *et al.* 1998). The extraction buffer included 43.5 mL ddH_20, 500 µL Tris Hcl (1 M PH 8.3), 5 mL KCl (0.5 M), 250 µL 1% Tween 20, 250 µL 1% NP40, and 500 µL Proteinase K solution (20 mg/mL). The Proteinase K solution included 0.5 mL glycerol, 0.5 mL ddH_20, and 20 mg Proteinase K. After being vortexed and briefly centrifuged (1000 RPM), samples were incubated at 50 degrees C for 4 hours. After

4 hours of enzyme activity, we denatured the Proteinase K by raising the temperature to 95 degrees C (3 minutes). The resulting DNA products were then frozen and stored for PCR.

PCR & Fragment Analysis: Next, we amplified 5 microsatellite loci in our DNA samples with PCR. We used primers designed by Fox (2004), including Dgm105, Dgm106, Dgm109, Dgm112, and Dgm112. Each PCR reaction used 6 µL Qiagen multiplex PCR mastermix, 1.2 µL of primer mix (2 mmol each), 3.8 µL ddH_20, and 1 µL DNA sample. PCR was run on a SimpliAmp Thermal Cycler. Cycling conditions were initiated with one cycle at 95 °C for 15 minutes, followed by 30 cycles (94 °C for 30 s, 58 °C for 180 s, 72 °C for 90 s) and a final extension at 72 °C for 10 minutes. Amplified DNA was diluted (1 µl amplified DNA and 10 µl ddH_20) and sent to the W.M. Keck Center for Comparative and Functional Genomics (University of Illinois at Urbana-Champaign Biotechnology Center, Urbana, IL, USA) for microsatellite fragment analysis. Alleles were called using GeneMapper™ software (Version Version 5: Applied Biosystems, Foster City, CA, USA). Finally, we identified genotypes of our samples by comparing their alleles with known alleles of our isoclonal lines maintained in the laboratory.

Repeated Measures Mixed Models

We analyzed changes in evolutionary variables during epidemics with repeated measures mixed models using the NLME package in R (Pinheiro & Bates 2000; R Core Team 2017). First, we summarized changes in genotype frequencies, including the four most frequently detected genotypes (Figs. S2 & S3; see Fig. 1 for each genotype's location in trait space) and all other genotypes pooled together (Fig. S4). Then, we calculated changes in mean focal host traits: competitive ability (Figs. 3 & S3) and susceptibility (Fig. 3). All models included tank as a random effect (random intercept and slope), standing trait variation (V) and time (t) as crossed fixed effects, and a parameter that allowed variance to change over time. This latter

parameter relaxed the assumption of homogeneity of variance and generally improved fits of model (via likelihood ratio tests).

Unfortunately, we could not fit comprehensive models that fully crossed standing trait variation (*V*), presence of parasites (*P*), presence of competitor/diluters (*C*), and time (*t*). Such models also generated undesirable complicated 4-way interactions. Thus, to both conserve statistical power and clarify our results, we used likelihood ratio tests to justify inclusion of presence/absence of parasites (*P*) or competitor/diluters (*C*) as crossed fixed effects (summarized in Table S1). We deviated from this model selection procedure twice. First, inclusion of parasites improved the model predicting the frequency of 'other' genotypes. However, since parasites were not significant as a main effect or interaction in the more complex model, we kept the simpler one. Second, both parasites and competitor/diluters independently improved the model predicting competitive ability. However, the model with both of these additional factors generated 4-way interactions and was not a significant improvement (via likelihood ratio test) of the model without competitor/diluters. Therefore, we present two complementary models predicting competitive ability. One includes parasites, is presented in the main text (Fig. 3), and reveals evolution during epidemics. The second one includes competitor/diluters, is presented below (Fig. S4), and reveals evolution before epidemics.

SUPPLEMENTAL RESULTS

Here, we present additional figures that complement the main text. We displaying the densities of competitor/diluters and their impact on infection prevalence (Fig. S1). Then we report selection of the repeated measures mixed models (Table S1) and display changes in genotype frequencies (Figs. S2 – S3) and impacts of competitors on competitive ability before epidemics. Finally, we present the eco-evolutionary impacts of final competitive ability on unscaled densities of focal hosts (Fig. S5), and demonstrate that the eco-evolutionary results are robust regardless of the time cutoffs used to define 'final ecological dynamics' (Table S3).

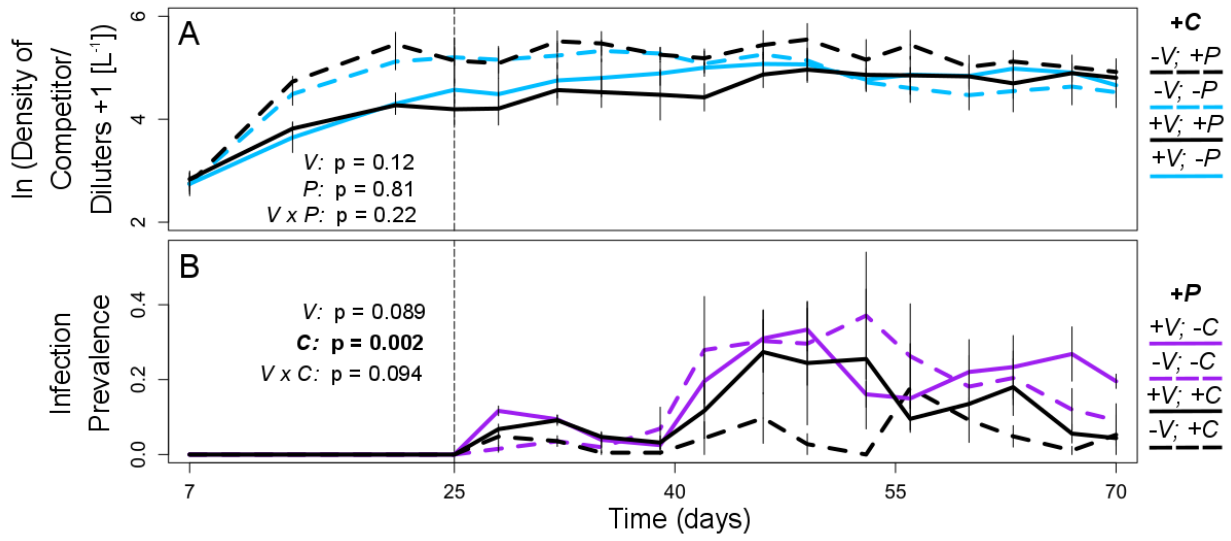

Figure S1. ***Diluters & Infection Prevalence:*** Epidemics begin after day 25 (vertical dashed line). The density of competitor/diluters and infection prevalence are integrated from days 25 to 70. **A)** Neither standing trait variation (*V*), parasites (*P*), nor their interaction significantly impacts the density of competitor/diluters. **B)** Their presence reduces infection prevalence, but it is not impacted by trait variaiton via a main effect or interaction. Abbreviations: *V* = standing trait variation (dashed = constrained; solid = variable); *P* = parasites (purple and black); *C* = competitor/diluters (blue and black). Error bars are standard errors.

Genotype Frequencies

Four genotypes dominated focal host populations: Midland 273, Warner 5, Dogwood 4, and Midland 263 (see Fig. 1 for their traits). We binned all other rarer genotypes together in a category of “Others.” The three infrequent genotypes with unknown traits (included in “Others”) represented, in aggregate, only 7% of individuals identified, including 3% identified from day 70. Initial genotype frequencies appeared relatively unimportant, since the genotype with highest initial mean frequency (19%) represented only 1% of individuals identified from day 70. In contrast, the genotype that dominated variable populations at the end of the experiment (Midland 273; 55%) started at a relatively low initial frequency (6%). Instead, selection imposed by interspecific competitors (Fig. S4) and especially parasites (Fig. 3) became more important.

Parasites drove changes in frequency of Midland 273, Midland 263, Warner 5, and Dogwood 4 (Fig. S2). Frequency of Midland 273 (the strongest competitor, only present in variable populations) increased slowly before epidemics (Fig. S2A). Then, parasites accelerated its increase during epidemics (Fig. S2B; P x t effect: $p < 0.0001$). Similarly, frequency of Midland 263 (the second-strongest competitor, only present in variable populations) also increased more steeply in parasite treatments during epidemics (Fig. S2D; $P \times t$ effect: $p = 0.013$). Frequency of Warner 5 (the strongest competitor in constrained populations) decreased before epidemics (Fig. S2E). Then, it increased during epidemics in constrained populations with parasites (Fig. S2F; V x P x t effect: $p = 0.0031$). Thus, these three genotypes all increased mean competitive ability during epidemics in their respective populations. In contrast, frequency of Dogwood 4 (a weaker competitor) initially increased (Fig. S2G), but declined or slowed as stronger competitors (panels A-F) replaced it during epidemics (Fig. S2H; P x t effect: $p = 0.0072$). These changes in genotype frequencies explain the evolution of competitive ability driven by parasites (Fig. 3).

Frequency of all other genotypes pooled together decreased uniformly before (Fig. S3A) and during epidemics (Fig. S3B; t effect: $p < 0.001$).

Competitor/diluters elicited more subtle changes in competitive ability (Fig. S4). Mean competitive ability started higher in variable populations (Fig. S4A). Then, at the onset of epidemics, it had become higher in treatments with competitor/diluters (Fig. S4B; *C* effect: p = 0.003), although only in variable populations (*V x C* effect: p = 0.029). These impacts of competitor/diluters faded during epidemics, as parasites drove stronger effects on competitive ability (Fig. 3).

Table S1. Model comparison identifies important predictors of genotype frequencies and mean traits during epidemics. Significant p values indicate improved fit (via likelihood ratio tests). Yes/no indicates whether the parameter was included in the final model. Final models are depicted graphically in Figs. S2–S3 (genotype frequencies) and Figs. 3 & S4 (traits).

Genotype	Figure Panel	Parasites **(*P*)**	Competitor/ Diluters **(*C*)**
Midland 273	S2B	p < 1e-4 (Yes)	p = 0.90 (No)
Midland 263	S3D	p = 0.02 (Yes)	p = 0.10 (No)
Warner 5	S2F	p < 0.01 (Yes)	p = 0.96 (No)
Dogwood 4	S2H	p < 1e-4 (Yes)	p = 0.10 (No)
Others (Pooled)	S3B	p = 0.03 (No)*	p = 0.11 (No)
Competitive Ability	*3B*	p < 1e-4 (Yes)	p = 0.03 (No)†
Competitive Ability	*S4B*	p < 1e-4 (No) †	p = 0.03 (Yes)
Susceptibility, β	*3D*	p < 0.01 (Yes)	p = 0.28 (No)

*Not included because yielded no new significant main effects or interactions

†Included in the complementary Competitive Ability model instead

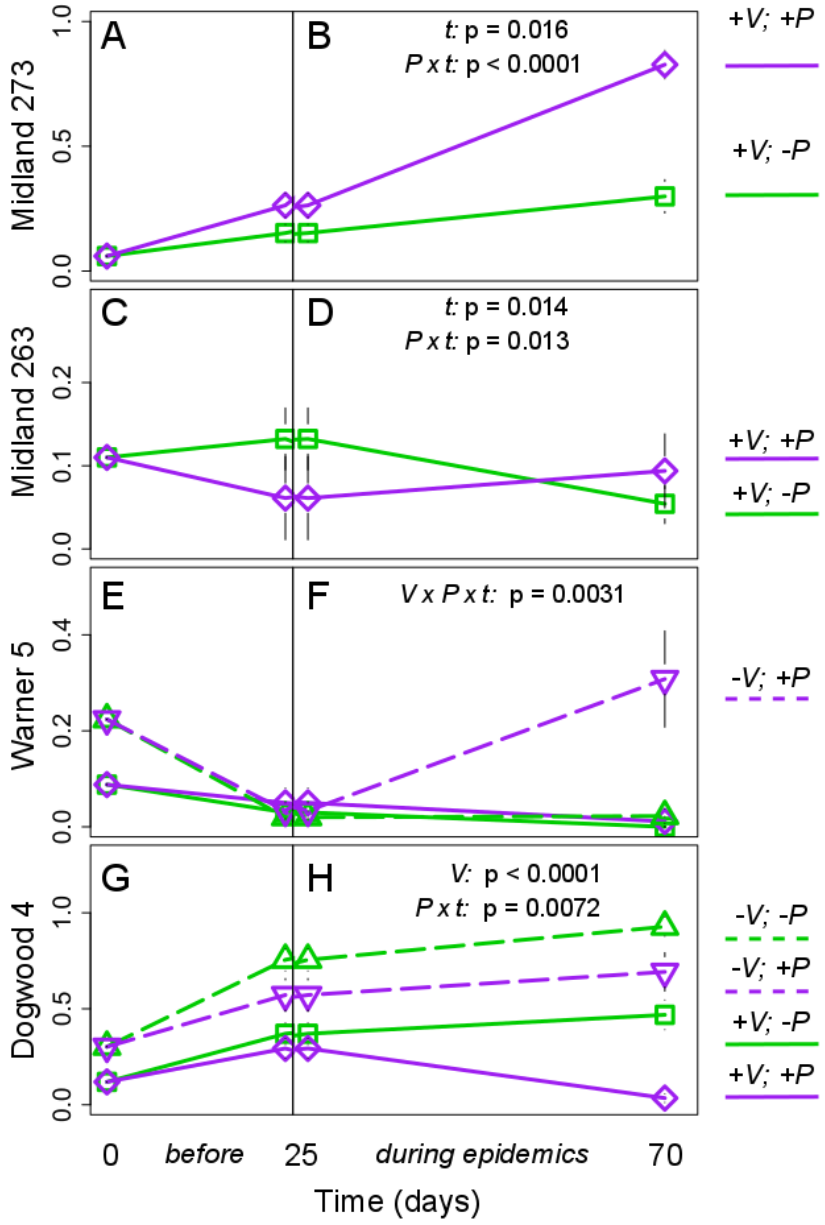

Figure S2. *Genotype Frequencies:* *Parasites drive changes in genotype frequencies.* P values (from repeated measures mixed models) indicate all significant changes during epidemics. The top three rows are all strong competitors in their respective populations. Frequency of Midland 273 **A)** initially increases and then **B)** parasites accelerate its increase during epidemics (purple [+*P*] vs. green [-*P*]). Frequency of Midland 263 in parasite treatments **C)** initially decreases but then **D)** increases during epidemics, especially relative to treatments without parasites. Frequency of Warner 5 **E)** initially decreases, but then **F)** it increases during epidemics in constrained treatments (-*V, +P*). In contrast, Dogwood 4 is a relatively weak competitor, especially in variable populations. Its frequency **E)** initially increases, but **F)** becomes replaced by the stronger competitors during epidemics. Abbreviations: *t* = time, *V* = standing trait variation; *P* = parasites. Error bars are standard errors; data include treatments with and without competitor/diluters.

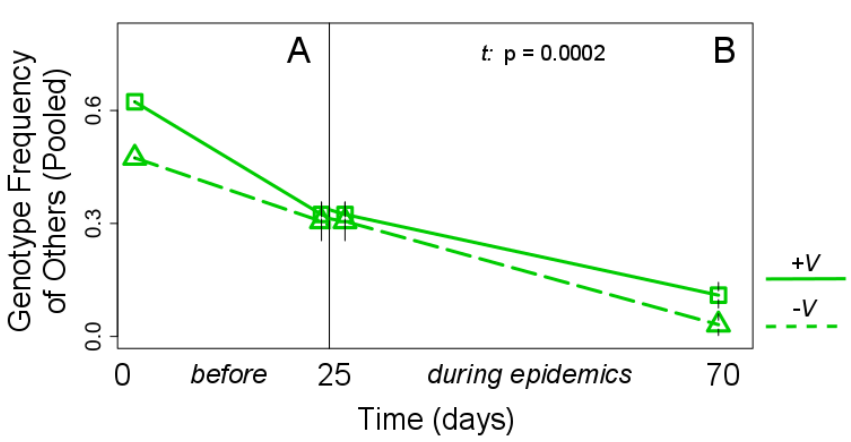

Figure S3. ***Other Genotype Frequencies:*** Frequency of all other genotypes pooled together decrease **A)** before and **B)** during epidemics. Abbreviations: *t* = time; *V* = standing trait variation. Error bars are standard errors; data include all treatments.

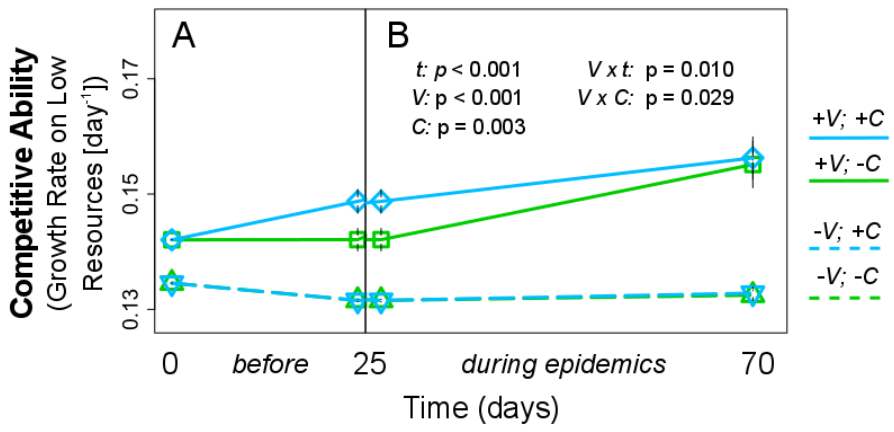

Figure S4. ***Evolution of Competitive Ability Before Epidemics:*** *Competitor/diluters elevate competitive ability, but only before epidemics.* P values (from repeated measures mixed models) indicate all significant effects. **A)** Mean competitive ability starts slightly higher in variable treatments. **B)** As epidemics begin, competitive ability in variable treatments has increased in treatments with competitor/diluters. However, as epidemics proceed, these effect disappears. These impacts of competitor/diluters likely become overshadowed by stronger impacts of parasites on competitive ability during epidemics (Fig. 3B). Competitor/diluters do not impact competitive ability in constrained populations. Abbreviations: *t* = time; *C* = competitor/diluters; *V* = standing trait variation. Error bars are standard errors; data include treatments with and without parasites.

Unscaled Densities of Focal Hosts

In the main text, we present the eco-evolutionary impacts of evolved competitive ability on the final density of focal hosts, scaled relative to competition- and disease-free baselines (Fig. 4). Here, we display the different baselines between variable and constrained populations and present the analogous eco-evolutionary impacts using absolute (i.e., unscaled) densities. The difference between the two metrics of 'host density' is driven by the higher baseline densities in constrained populations, even after 3-5 generations of ecological dynamics. We are currently developing theory that couples consumer-resource and eco-evolutionary dynamics to better study this result. The percent of juveniles (vs. adults) was also much higher in constrained populations, which could contribute to the differences in baseline densities (preliminary evidence not presented). Given this intriguing result, the scaled densities presented in the main text (Fig. 4) seem the most appropriate metric for asking how rapid evolution buffers the densities of hosts from competition and disease. Nevertheless, these unscaled densities provide a complementary perspective.

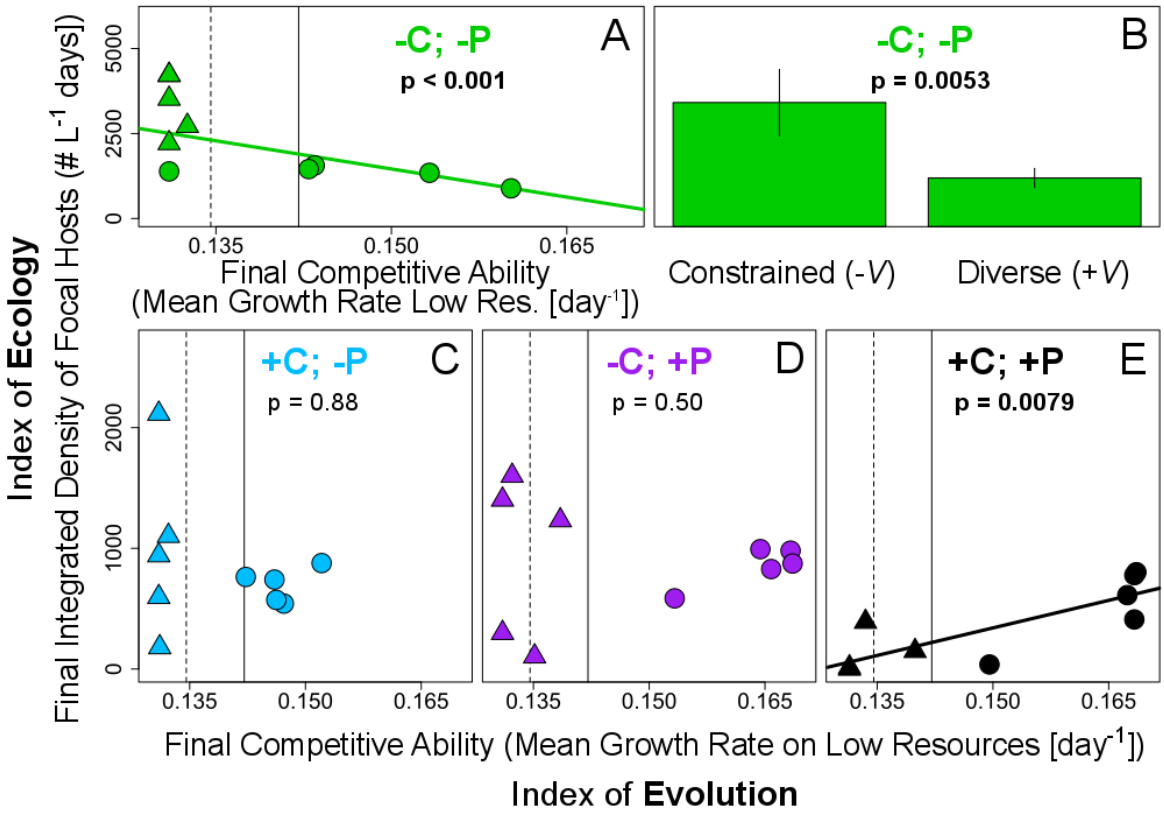

Figure S5. ***Buffering Unscaled Densities:*** *Rapid evolution of competitive ability lowers baseline density of focal hosts, but still rescues absolute density in treatments with both competitor/diluters and parasites.* Vertical lines indicate initial mean competitive ability (dashed = constrained; solid = variable). Final density of focal hosts (an index of ecology) is integrated during the last three weeks for constrained (triangles) and variable (circles) treatments. **A)** Higher final competitive ability—an index of evolution—lowers absolute density in treatments without competitor/diluters or parasites (-C, -P). **B)** Thus, baseline densities are higher in constrained treatments (-*V*). These different baselines standardize final relative densities of focal hosts (Fig. 4). Higher final competitive ability has no impact on absolute (i.e., unscaled) density in treatments with only **B)** competitor/diluters (+*C, -P*) or **C)** parasites (-*C, +P*), but **D)** elevates it in treatments with both (+*C, +P*). Key to abbreviations: *C* = competitor/diluters; *P* = parasites; *V* = standing trait variation.

Robust Eco-Evolutionary Results

Table S3. Eco-evolutionary results are qualitatively robust to different cutoffs for 'final ecological dynamics' (i.e., dynamics integrated over the final 17, 21, or 24 days of the experiment).

Dependent Variable	Figure Panel	Treatment (Statistical Test)	Integration Cutoff (days)	P Value(s)
Final Scaled Density of Focal Hosts	Fig. 4A	+*C*, -*P* (regression)	17	p = 0.031
			21*	p = 0.026
			24	p = 0.029
	Fig. 4B	-*C*, +*P* (regression)	17	p = 0.0028
			21*	p = 0.0016
			24	p = 0.0011
	Fig. 4C	+*C*, +*P* (regression)	17	p = 0.0033
			21*	p = 0.0036
			24	p = 0.00037
Final Absolute Density of Focal Hosts	Fig. S5A	-*C*, -*P* (regression)	17	p = 0.0003
			21*	p = 0.0003
			24	p = 0.0003
	Fig. S5B	-*C*, -*P* (t-test)	17	p = 0.0079
			21*	p = 0.0079
			24	p = 0.024
	Fig. S5C	+*C*, -*P* (regression)	17	p = 0.68
			21*	p = 0.88
			24	p = 0.96
	Fig. S5D	+*C*, -*P* (regression)	17	p = 0.68
			21*	p = 0.50
			24	p = 0.28
	Fig. S5E	-*C*, +*P* (regression)	17	p = 0.0097
			21*	p = 0.0079
			24	p = 0.0083

* Final 21 day cutoffs are depicted in figures

REFERENCES

1.

Bolker, B.M. (2008). *Ecological Models and Data in R*. Princeton University Press.

2.

Fox, J.A. (2004). New microsatellite primers for *Daphnia galeata mendotae*. *Molecular Ecology Notes*, 4, 544-546.

3.

Grover, J.P. (1997). *Resource Competition*. Chapman & Hall.

4.

Hall, S.R., Becker, C.R., Duffy, M.A. & Caceres, C.E. (2012). A power-efficiency trade-off in resource use alters epidemiological relationships. *Ecology*, 93, 645-656.

5.

Hall, S.R., Sivars-Becker, L., Becker, C., Duffy, M.A., Tessier, A.J. & Cáceres, C.E. (2007). Eating yourself sick: transmission of disease as a function of foraging ecology. *Ecol. Lett.*, 10, 207-218.

6.

Lampert, W. & Trubetskova, I. (1996). Juvenile growth rate as a measure of fitness in *Daphnia*. *Funct. Ecol.*, 10, 631-635.

7.

Pinheiro, J. & Bates, D. (2000). *Mixed-Effects Models in S and S-PLUS*. Springer New York.

8.

R Core Team (2017). R: A language and environment for statistical computing. R Foundation for Statistical Computing Vienna, Austria.

9.

Schwenk, K., Sand, A., Boersma, M., Brehm, M., Mader, E., Offerhaus, D. *et al.* (1998). Genetic markers, genealogies and biogeographic patterns in the cladocera. *Aquatic Ecology*, 32, 37-51.

10.

Strauss, A.T., Bowling, A.M., Duffy, M.A., Cáceres, C.E. & Hall, S.R. (in revision). Linking host traits, interactions with competitors, and disease: Mechanistic foundations for disease dilution. *Funct. Ecol.*